Soft Matter

PAPER

View Article Online
View Journal | View Issue

Cite this: *Soft Matter*, 2024, **20**, 8373

Emulsifying mechanisms of phospholipids in high-pressure homogenization of perfluorocarbon nanoemulsions†

Larissa J. Lubitz, [abc] Harden Rieger[ab] and Gero Leneweit*[abc]

Phospholipids are the most ubiquitous emulsifiers in foods, beverages, pharmaceuticals, and human physiology, but their emulsifying properties are extremely complex. Differential analyses of mechanisms contributing to their functionality are presented in a modular approach. Addition of cholesterol to a natural phospholipid blend disturbs emulsification beyond specific thresholds for size, polydispersity and formation of emulsifying monolayers. Beyond a ratio of lipid concentration to dispersed volume of 1 mM per 1% (v/v) of perfluorocarbon (PFC), phospholipids no longer form monolayers but instead form triple layers that emulsify the PFC. Using synthetic saturated phospholipids, it can be shown that emulsification is most successful for fatty acids closely below their main transition temperature. Phospholipid head groups are more effective for emulsification the more they increase the area per molecule or the zeta potential. Including a comparison with literature results, it can be shown that high molecular weight emulsifiers like proteins are not dependent on the ratio of viscosities η of the dispersed phase to the continuous phase, η_D/η_C. In contrast, smaller molecular weight emulsifiers like phospholipids show a mild increase in effectiveness with rising η_D/η_C, although this increase is not as strong as that observed for low molecular weight detergents. Ruptures of highly resistant emulsifying interfacial layers obviously lead to direct droplet break-up, irrespective of the resistance of a high-viscosity droplet. The lower the break-up resistance of an emulsifier, the more is it governed by the bulk viscosity of the dispersed phase. Our results allow the preparation of a phospholipid-stabilized emulsion with optimized emulsification settings for pharmaceutical applications.

Received 9th July 2024,
Accepted 3rd September 2024

DOI: 10.1039/d4sm00828f

rsc.li/soft-matter-journal

Introduction

For decades, the food, beverage, and pharmaceutical industries have optimized the attributes of their products through the use of high-pressure homogenization.[1–3] Because phospholipids are widely used as biocompatible emulsifiers and liposomes as vesicles for widespread delivery of active substances in food and medicine, it is worth investigating both. However, most naturally occurring lipid emulsion systems, such as triglycerides, triterpenes or other biogenic organic phases dispersed in water do not form stable nanoemulsion systems. Instead, complex gel-forming aggregates such as organogels or hydrogels can be formed due to the complexity of possible interactions with phospholipids,[4] resulting in various instabilities in phospholipid emulsion systems.[5] To prevent gel formation with phospholipids, we used ommiphobic excipients with no measurable solubility for phospholipids – perfluorocarbons (PFCs). These are an ideal model system for the emulsification properties of phospholipids. In addition, they find increasing use both as pharmaceutical excipients and in medical applications. For instance, they are applied in ^{19}F magnetic resonance imaging. Due to the high gas-binding capability of PFCs, emulsions containing such substances have been tested as artificial blood substitutes or oxygenated carriers for organ transplants.[6] In these mentioned cases, PFC/W nanoemulsions were used as pharmaceutical end products, but they can also be used as intermediates for the production of asymmetric liposomes. In these liposomes, the inner and outer bilayer leaflets have a different composition, *i.e.* asymmetric composition. Pautot *et al.* (2003) generated asymmetric liposomes by centrifuging a water-in-oil emulsion into a water phase enriched with phospholipids, following the technique disclosed by Träuble and Grell in 1971.[7,8] Asymmetric liposomes offer the advantage of an increased encapsulation

[a] *ABNOBA GmbH, Allmendstr. 55, Niefern-Öschelbronn 75223, Germany. E-mail: gero.leneweit2@kit.edu*
[b] *Carl Gustav Carus-Institute, Association for the Promotion of Cancer Therapy, Niefern-Öschelbronn 75223, Germany*
[c] *Karlsruhe Institute of Technology (KIT), Institute of Mechanical Process Engineering and Mechanics, Straße am Forum 8, Karlsruhe 76131, Germany*

† Electronic supplementary information (ESI) available. See DOI: https://doi.org/10.1039/d4sm00828f

efficiency compared to symmetric ones. Conventional liposome manufacturing techniques demonstrated encapsulation efficiencies of less than 50% for high molecular weight molecules.[9–12] Liposomes based on a water-in-perfluorocarbon nanoemulsion instead can reach an encapsulation efficiency of more than 90%, as demonstrated by Ullmann *et al.* in 2021.[13] Optimization of all practical applications needs a much deeper understanding of the complex interactions and mechanisms of phospholipid and cholesterol dynamics at the interfaces. This goal is pursued using a modular approach in the present study. Concerning the further use of the PFC/W nanoemulsion for the preparation of asymmetric liposomes, the incorporation of cholesterol is of enormous importance for mimicking cellular[14,15] structures. Cholesterol can positively affect the droplet size distribution and stability through interactions within the bilayer.[16,17] Cholesterol can be incorporated into phospholipid bilayers at concentrations of up to 50 mol%.[18,19] Therefore, the influence of different molar cholesterol contents is investigated here.

Not only the percentage of cholesterol but also the total concentration of lipids in relation to the dispersed phase volume has a decisive influence on the resulting emulsion. A fast and sufficient supply of emulsifier molecules concurrently with the break-up of the emulsion droplets ensures the stabilization of newly generated interfaces. Calculations of the surface area per molecule allow an assessment of whether emulsion droplets are surrounded by a monolayer or a multilayer of lipids. Hildebrandt *et al.* (2016) found multilayers at the squalene–water interface using profile analysis tensiometry, while Tikhonov (2020) proved the existence of DPPC and DSPC multilayers at the silica–water interface.[14,15] However, the formation of phospholipid monolayers *vs.* multilayers is not yet proven in a nanoemulsion system. Another important aspect of emulsion stabilization is the emulsifier itself, where phospholipids can be varied in two ways: first the acyl chain length of the fatty acids and second the hydrophilic head group. Nii and Ishii (2005) showed for triglyceride emulsions that longer chain lengths cause an increase in particle size.[20] Much less obvious is the influence of the phospholipid head group on the resulting emulsion characteristics. Kleinschmidt and Tamm (2002) investigated the threshold between micelle-forming and bilayer-forming phospholipid species.[21] This threshold not only depends on the fatty acid chain length but even more importantly on the physicochemical characteristics of the head group. They were able to show that the limit lies between 6 C atoms (for phosphatidylethanolamine) and 12 C atoms (for phosphatidyl-glycerol). However, the effect of the head group on the emulsifying properties of phospholipids has not yet been studied.

Focusing also on the dispersed phase, it is useful to vary the perfluorocarbon species to study the influence of the viscosities of dispersed and continuous phase more closely. Qian *et al.* (2011) showed that a reduced viscosity ratio between the dispersed phase η_D and continuous phase η_C leads to a smaller droplet size.[22] Similarly, Tesch and Schubert (2002) and Behrend and Schubert (2000) showed that an increase in the viscosity of the continuous phase, resulting in a reduction of the viscosity ratio η_D/η_C, leads to an avoidance of the coalescence of particles, as the squeezing out of the continuous phase between two particles is delayed.[23,24]

Following our previous study that focused on the flow conditions during high-pressure homogenization and process optimization for a PFC/W nanoemulsion,[25] the present study analyses all mentioned formulation parameters to elucidate their effect on emulsification. The modular approach of studying each parameter in a singular variation scheme aims to contribute to the basic understanding of the various functionalities. As phospholipids are neither soluble in the aqueous phase nor in the perfluorocarbon phase, they are introduced in liposomal conformation. After emulsification, a mixture of nanoemulsion droplets and remaining phospholipid liposomal bilayers coexist in the formulations. To enable their detailed analysis, differential centrifugal sedimentation in a sucrose gradient is applied to allow an undisturbed view on separated nanoemulsion droplets, fractionated in different sizes for accurate quantification.

Experimental section

Materials

Purified egg yolk phospholipid containing ~80% phosphatidylcholine (E80) as well as 1,2-dimyristoyl-*sn-glycero*-3-phosphocholine (DMPC), 1,2-dipalmitoyl-*sn*-glycerol-3-phosphocholine (DPPC), 1,2-distearoyl-*sn-glycero*-3-phos-phocholine (DSPC), 1,2-dipalmitoyl-*sn-glycero*-3-phosphogly-cerol (sodium salt, DPPG-Na), 1,2-dipalmyitoyl-*sn-glycero*-3-phophate (DPPA) and 1,2-dipalmitoyl-*sn-glycero*-3-phospho-ethanolamine (DPPE) were received from Lipoid GmbH (Ludwigshafen, Germany) as a gift. Monosodium phosphate dihydrate ($NaH_2PO_4{\cdot}2H_2O$), disodium phosphate dihydrate ($Na_2HPO_4{\cdot}2H_2O$), D(+)-saccharose, hydrochloric acid (37% fuming), and cholesterol (Chol) were obtained from Carl Roth GmbH & Co. KG (Karlsruhe, Germany) and were of pharmaceutical quality (Ph. Eur.). Perfluoroperhydrophenanthrene (PPHP), perfluoroheptane and per-fluoro-1,3-dimethylcyclohexane were obtained from F2 Chemicals Ltd (Preston, Lancashire, United Kingdom). Perfluorodecalin and perfluorooctyl bromide were obtained from abcr GmbH (Karlsruhe, Germany).

Methods

Preparation of buffer and sucrose solutions

In order to prepare the emulsion, 10 mM phosphate (6.08 mM $Na_2HPO_4{\cdot}2H_2O$ and 3.92 mM $NaH_2PO_4{\cdot}2H_2O$) was utilized as the buffer, and 1 M hydrochloric acid was used to adjust the pH to 7.4. Throughout the whole manufacturing process, the buffer was sterile-filtered and degassed.

The sucrose solutions (20%, 30%, 40%, 50%, and 60% (w/v)) were made by weighing the necessary amount of sucrose, adding the appropriate volume of deionized water, and then filtering the mixture through a 0.45 μm syringe filter (Carl Roth GmbH & Co. KG, Karlsruhe, Germany).

Preparation of the PFC/W nanoemulsion

The phospholipid and cholesterol mixtures were first prepared as a lipid film with a concentration of 150 mM utilizing the thin-film approach in order to prepare the PFC/W nanoemulsions. Each emulsion batch was diluted to the desired lipid concentration for additional processing after the lipid film had been rehydrated with buffer to create a 150 mM lipid stock solution. Using Ultra-Turrax® at 8000 rpm for five minutes, high shear mixing was used to pre-crush and disperse the lipid vesicles in the buffer. The pre-emulsion was then created by adding the required amount and species of perfluorocarbon and mixing once more with Ultra-Turrax® for ten minutes at 15 000 rpm. Subsequently, the pre-emulsion was filled into a syringe and processed by Microfluidizer LV1 (Microfluidics, Westwood, USA), which was utilized in conjunction with two interaction chambers (F12Y 75 μm and H20Z 200 μm). The emulsion was homogenized for six cycles at 1000 bar, while the process housing was cooled. An argon environment was used for the entire emulsion generation process utilizing Ultra-Turrax® and Microfluidizer LV1 to prevent lipid oxidation.

Separation of liposomes and PFC-droplets

A sucrose gradient was used for the analytical separation of the residual liposomes and the size-based separation of the PFC droplets. In order to do this, sucrose solutions were placed in a 15 mL tube, with a total capacity of 8.2 mL, on top of each other in ascending concentration. Afterwards, 0.8 mL of the PFC/W nanoemulsion was stacked dropwise on top and the tube was centrifuged for 30 minutes at 4000 × g in a swinging-bucket rotor. Then, nine fractions, each containing 1 mL, were carefully taken from the top and placed straight into a disposable semi-micro cuvette made of polystyrene (Carl Roth GmbH & Co. KG, Karlsruhe, Germany) to be analyzed using dynamic light scattering. The remaining liposomes in the PFC/W nanoemulsion are assessed by considering the count rate percentages of fractions 1 and 2.[25]

Data presentation and statistical analysis

The data are presented as an arithmetic mean with standard deviation for each experiment, which was carried out in triplicate. A two-sample t-test with equal variances was conducted after a single factor analysis of variance (ANOVA) at a significance level of $p < 0.05$ to assess the data statistically. Microsoft Excel (Reymond, WA, USA) was used for all analyses.

Results and discussion

Experimental investigation of changes in the emulsifier formulation

Variation of the cholesterol percentage. To prepare perfluorocarbon-in-water (PFC/W) nanoemulsions, a pre-emulsion must first be prepared using Ultra-Turrax® at 15 000 rpm for 10 minutes. This pre-emulsion, consisting of the perfluorocarbon (PFC, 2.5% v/v) in a phosphate-buffered phospholipid/cholesterol suspension, was further emulsified by six consecutive runs through the homogenization chamber, also referred to as cycles, at 1000 bar. The phospholipid component was egg yolk phospholipid with at least 80% phosphatidylcholine (E80), where the test series focused on varying the corresponding cholesterol content x_{chol} from x_{chol} = 5 mol% to 40 mol%, as this reflects the physiologically and pharmaceutically relevant range (Table 1 and Fig. 2 part 1). The results of this variation of the cholesterol content are shown in Fig. 1 and Fig. S1 (ESI†).

Considering the resulting PFC droplet size (Z-average, Fig. 1a), it can be observed that there is an increasing trend of the Z-Ave with increasing cholesterol content, starting from 10 mol%. The cholesterol dependence of the polydispersity index (PdI) in Fig. 1b, on the other hand, shows a minimum of the PdI at 20 mol% with 0.320 ± 0.010 and an increase up to 0.470 ± 0.069 at 40 mol%. The derived count rate can be assumed as a relative measure of the number of particles in the emulsion. The DCR shows a maximum at 5 mol% with 5281 kcps ± 94 kcps (Fig. 1c). A comparison of the count rates from 10 mol% to 40 mol% shows a slightly increased droplet count at 20 mol% with 4223 kcps ± 196 kcps. To evaluate the final PFC/W emulsion, it is important to remove any remaining liposomes from the phospholipid stock suspension derived from the emulsion. For this purpose, an analytical sucrose gradient with pre-layered sucrose solutions of 20% to 60% (w/v) is used. After centrifugation for 30 minutes at 4000 × g and separation into 9 fractions starting from the top, the liposomes remain in the first two fractions due to their density. For a rough estimate of the proportion of liposomes, the sum of the count rate percentages from both fractions is therefore considered (Fig. 1c). There is a linear increase of liposomes in a PFC/W nanoemulsion from 20 mol% to 60 mol%.

In total, Fig. 1 shows that an increasing cholesterol content in PFC droplets dispersed in water emulsified by lipids leads to larger particles, a higher PdI for $x_{chol} > 30$ mol% and lower particle yields for $x_{chol} > 5$ mol%. Moreover, the emulsification yield, *i.e.* the conversion rate of phospholipids in bilayer

Table 1 Chemical composition of emulsions under study

Experimental investigation	Lipids	Composition [mol%]	Lipid concentration [mM]	Type of PFC and percentage % (v/v)
Variation of cholesterol percentage	E80/Chol	$(100 - X):X^a$	7.5 mM	PPHP, 2.5% (v/v)
Variation of the total lipid concentration	E80/Chol	95 : 5	Y mM^b	PPHP, 2.5% (v/v)
Variation of the fatty acid chain length	DXPC/Chol	60 : 40	7.5 mM	PPHP, 2.5% (v/v)
Variation of the phospholipid head group	DPPX/Chol	60 : 40	7.5 mM	PPHP, 2.5% (v/v)
Variation of the volume of dispersed phase	E80/Chol	95 : 5	7.5 mM	PPHP, Z% (v/v)^c
Variation of the perfluorocarbon species	E80/Chol	60 : 40	7.5 mM	PFC; 2.5% (v/v)

^{a} X = 5/10/20/30/40 mol%. ^{b} Y = 2.5/5/7.5/15 mM. ^{c} Z = 2.5/5/10% (v/v).

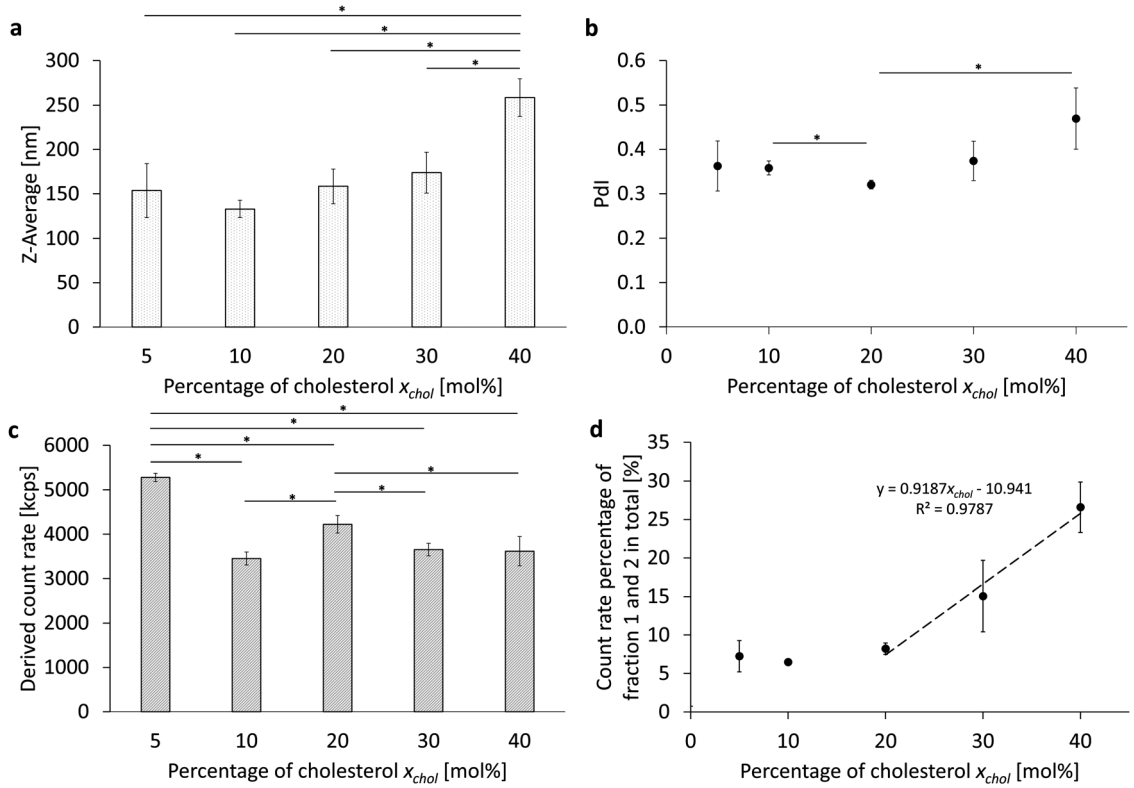

Fig. 1 Comparison of the different percentages of cholesterol. (a) The *Z*-average (*Z*-Ave) after 6 cycles at 1000 bar without fractionation using a sucrose gradient, (b) the corresponding polydispersity index (PdI), (c) the corresponding derived count rate (DCR) of the PFC/W nanoemulsion and (d) the count rate percentages of fraction 1 and 2 after separation using a sucrose gradient. The bars or dots represent the mean values ± SD. A one-way ANOVA followed by a two-sample *t*-test assuming equal variances was performed at a significance level of $*p < 0.05$; $n = 3$.

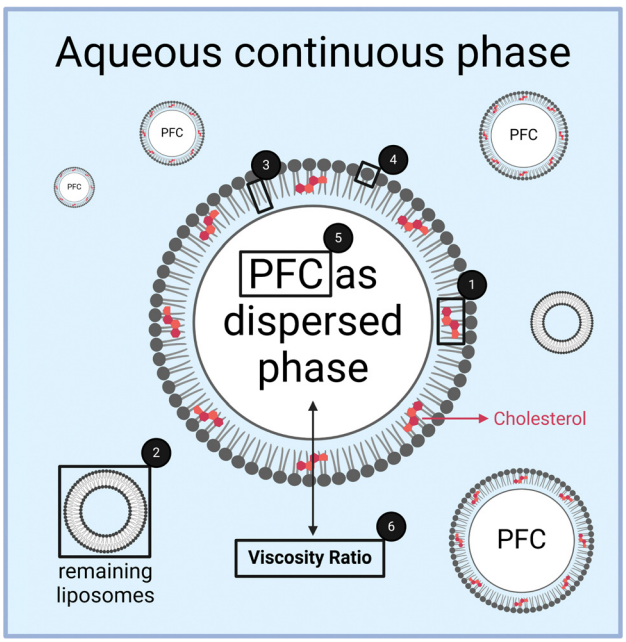

Fig. 2 Schematic illustration of the 6 different experimental investigations as detailed in Table 1. (1) Variation of the cholesterol content, (2) variation of the total lipid concentration, (3) variation of the phospholipid fatty acid chain length and (4) head group, (5) variation of the volume of the dispersed phase and (6) variation of the PFC species to vary the viscosity ratio between both phases.

conformation transformed into emulsifying monolayers is much lower for $x_{chol} > 20$ mol%.

Variation of the total lipid concentration

Analogous to the variation of the cholesterol content, the total lipid content c_L was varied from $c_L = 2.5$ mM to 15 mM in the PFC/W nanoemulsion in another parameter study (Table 1 and Fig. 2 part 2). The results are shown in Fig. 3 and Fig. S2 (ESI†). A significant minimum in the *Z*-averaged emulsion drop size (*Z*-Ave) at $c_L = 5$ mM with a *Z*-Ave = 124 nm ± 5 nm can be seen in Fig. 3a; the resulting droplet sizes are shown before the separation of the nanoparticle species and sizes in a sucrose gradient (Fig. 3a). This *Z*-Ave minimum at $c_L = 5$ mM is about 12.1% smaller than the mean *Z*-Ave of all other c_L. A similar result can also be seen in the change of the PdI in relation to the lipid concentration (Fig. 3b). Here, too, there is a minimum of PdI at 5 mM with 0.247 ± 0.008, which is about 10.5% smaller than the mean of all other PdI. For the derived count rate (DCR, Fig. 3c), there is a linear relationship between the DCR and the total lipid concentration from 2.5 mM to 7.5 mM. This relationship indicates two independent processes: for $c_L <$ 5 mM, there is a shortage of emulsifier, leading to increased drop sizes. For $c_L > 5$ mM, there is an excess of emulsifier, leading to a relative increase in lipids forming bilayers (*i.e.* liposomes), no longer leading to an increase of emulsifying

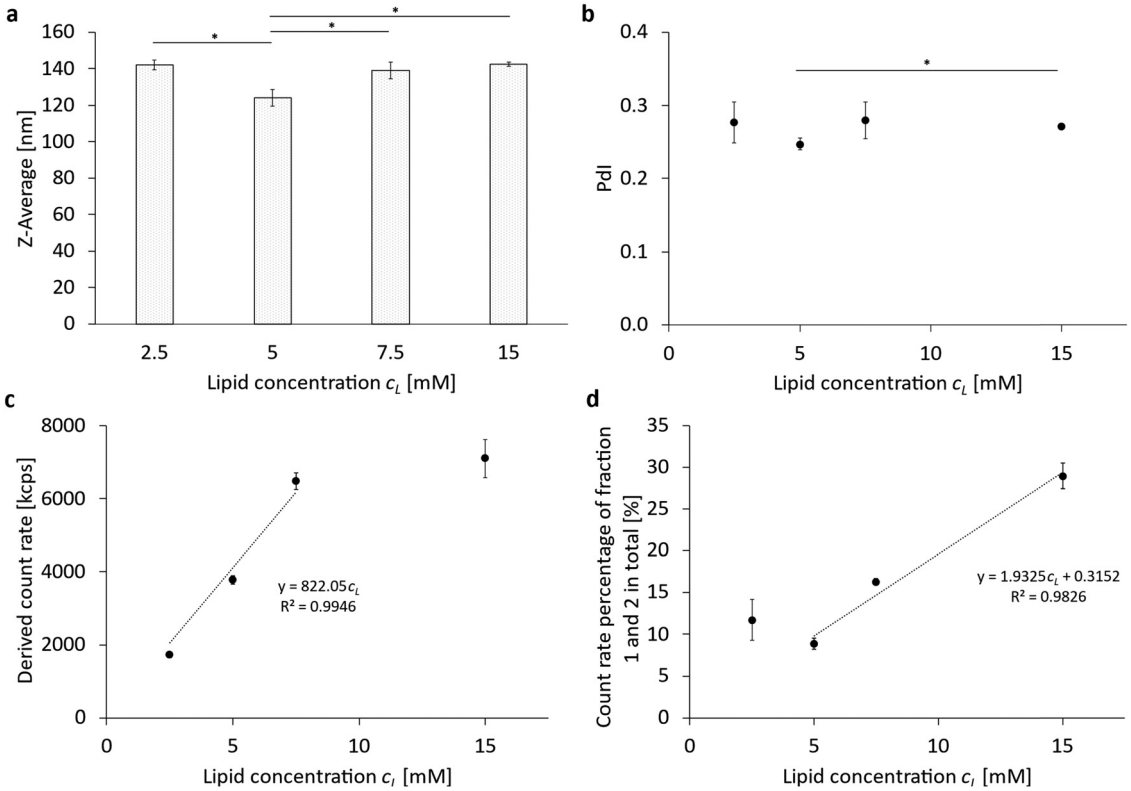

Fig. 3 Comparison of the different total lipid concentrations. (a) The *Z*-average (*Z*-Ave) after 6 cycles at 1000 bar without fractionation using a sucrose gradient; (b) the corresponding polydispersity index (PdI), (c) the corresponding derived count rate (DCR) of the PFC/W nanoemulsion and (d) the count rate percentages of fraction 1 and 2 after separation using a sucrose gradient. The bars or dots represent the mean values ± SD. A one-way ANOVA followed by a two-sample *t*-test assuming equal variances was performed at a significance level of $*p < 0.05$; $n = 3$.

monolayers because of the saturation of the droplet surfaces. This can be seen when considering the count rate percentage of fractions 1 and 2 in total, as shown in Fig. 3d. Table 2 shows a comparison of lipid molar concentrations with a hypothetical surface area per molecule, calculated by the total surface area of all fractions of emulsion droplets with their fraction-specific size of the *Z*-Ave and the total volume fraction of the disperse phase, divided by the molar concentration of phospholipids. For the phospholipids, fractions 1 and 2 are discounted as they do not contribute to emulsification as they persist in their liposomal conformation. Moreover, we apply a yield of 72.48% of the phospholipids contributing to emulsification, based on phospholipid analysis. For $c_L \geq 5$ mM, a linear relationship with the total lipid concentration is visible which means that doubling c_L leads to a doubling of the relative amount of liposomes among the nanoparticles. The calculation of the hypothetical surface area per molecule is presented in detail in Table S7 (ESI†).

Table 2 Surface area depending on lipid concentration, considering a minimum surface area per molecule comparable to POPC with 71.0 Å^2 per molecule (Klapper *et al.*, 2013)[26]

Lipid concentration [mM]	Hypothetical surface area per molecule [Å^2 per molecule]
2.5	85.56
5	39.85
7.5	26.36
10	27.69

We approximate the natural blend of the egg yolk phosphatidylcholine E80 by POPC molecules, which have been shown to possess a surface area of about 71.0 Å^2 per molecule.[26] Therefore, we have to assume that only for the lowest lipid concentration $c_L = 2.5$ mM, a lipid monolayer is formed which is slightly less dense than a phospholipid bilayer of POPC. For $c_L \geq 7.5$ mM, the emulsifiers apparently form lipid multilayers. The existence of such multilayers has been proven recently for DPPC and DSPC.[15] Since phase boundaries between hydrophilic and hydrophobic phases need an odd number of amphiphilic layers, we have to conclude that multilayers with 3 monolayer leaflets are formed for $c_L \geq 7.5$ mM, while for c_L = 5 mM, an inhomogeneous coating of monolayers and triple-layers has to be expected.

In summary, the phospholipid concentration c_L has an optimum of around 5 mM for achieving minimum droplet size and PdI and maximum emulsification for the given volume V_D of the disperse phase, which is $V_D = 2.5\%$ (v/v). In general terms, this means that a ratio of c_L/V_D = 2 mM/1% (v/v) creates an optimum in emulsification efficiency and minimum droplet size and PdI. Calculations of the total mass of lipids emulsifying PFC droplets allow to conclude that emulsification is only in a monolayer conformation for c_L/V_D = 1 mM/1% (v/v) but

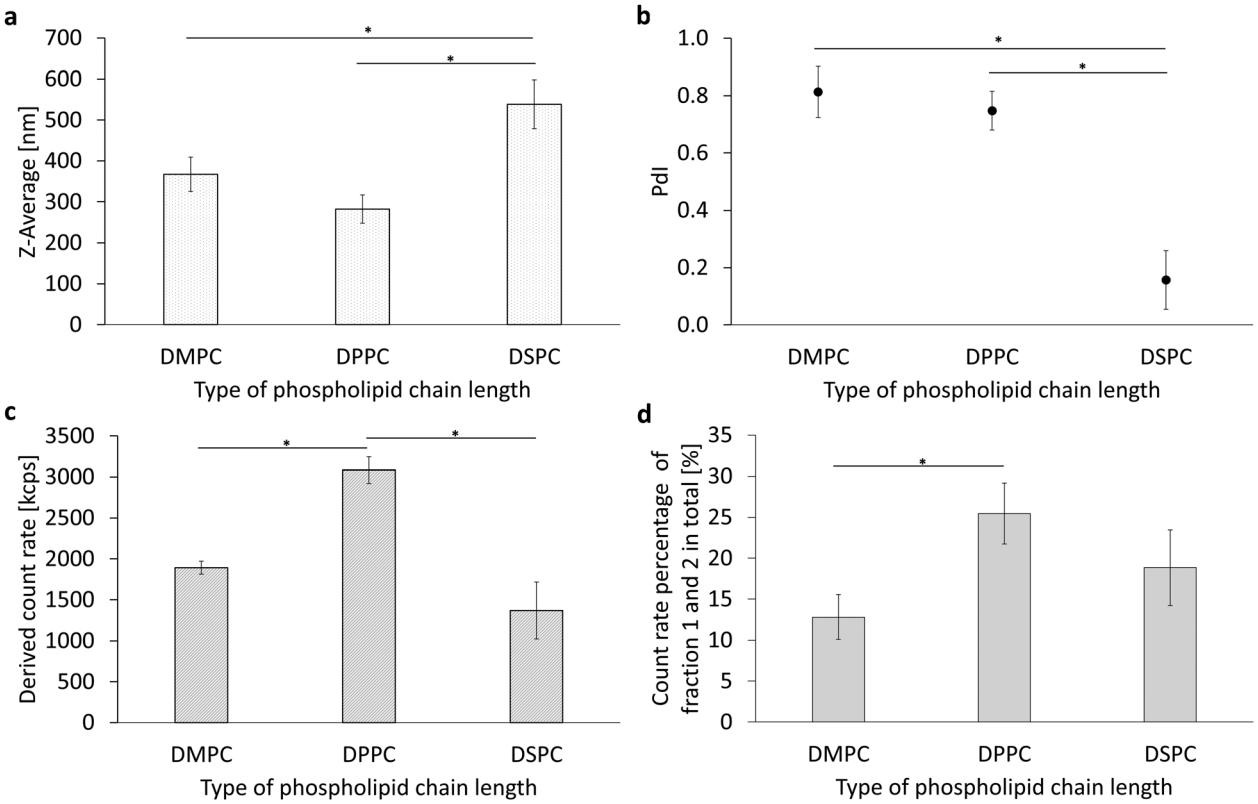

Fig. 4 Comparison of the different phospholipid chain lengths from 14 to 18 carbon atoms per fatty acid. (a) The *Z*-average (*Z*-Ave) after 6 cycles at 1000 bar without fractionation, (b) the corresponding polydispersity index (PdI), (c) the corresponding derived count rate (DCR) of the PFC/W nanoemulsion and (d) the count rate percentages of fractions 1 and 2 after centrifugation in a sucrose gradient. The bars represent the mean values with the standard deviation as error bars. A one-way ANOVA followed by a two-sample *t*-test assuming equal variances was performed at a significance level of $*p < 0.05$; $n = 3$.

forms either inhomogeneous mixtures of mono and triple layers or homogeneous triple layers for $c_L/V_D \geq 2$ mM/1% (v/v).

Variation of the phospholipid chain length and head group

In another investigation of the various parameters for the formulation of a PFC/W nanoemulsion, the emulsifier itself was varied. On the one hand, the head group of the phospholipid was varied with a constant saturated fatty acid chain length (Table 1 and Fig. 2 part 4) and on the other hand, the reverse case was studied in which the saturated fatty acid chain length was varied with a constant phospholipid head group (Table 1 and Fig. 2 part 3). The phospholipids were selected in relation to already approved pharmaceutical products. Since the studies shown in Fig. 1 and 3 were performed with the natural phospholipid blend E80 (containing 80% egg yolk phosphatidylcholines and 20% non-cholines), different results have to be expected regarding size ranges, PdI, and count rates.

The results of the chain length variation are summarized in Fig. 4 and Fig. S3 (ESI†). There is a significant maximum particle size (*Z*-Ave, Fig. 3a) for DSPC with 508 nm ± 58 nm. The differences between the shorter-chain phospholipids DMPC and DPPC in terms of particle size and polydispersity (Fig. 4b) are not yet significant with the given number of samples tested ($n = 3$) but a trend for a minimum size for DPPC is visible. However, DSPC shows a significant minimum for the PdI with 0.157 ± 0.102. The derived count rates (DCRs) shown in Fig. 3c show very strong differences between the chain lengths with DPPC being more than doubled compared to DSPC and >50% higher than DMPC. The results shown in Fig. 3c are consistent with those in Fig. 3a because smaller *Z*-Ave necessarily leads to higher count rates at equal volumes of the dispersed phase. The count rate percentages of fractions 1 and 2 shown in Fig. 4d reveal a significant difference between DMPC and DPPC. It reflects the fact that DMPC is in the fluid phase under the processing conditions, while DPPC is in the gel phase in both monolayer and bilayer conformation. High-pressure homogenization at room temperature (20 °C) leads to a temperature increase due to friction with a final temperature of the nanoemulsion of about 25.8 °C under the processing conditions of 1000 bar, measured by infrared thermometry at the outlet. This is enough to keep the emulsion above the main transition temperature T_m for DMPC (T_m = 24 °C) during processing from the microfluidic channel to the outlet but insufficient for DPPC (T_m = 41 °C) and DSPC (T_m = 55 °C). The theoretical friction-generated heat by the processing conditions of 1000 bar is 2.41 K per cycle, *i.e.* 14.47 K in 6 consecutive homogenization runs. Thus, >50% of the generated heat is conducted to the stainless steel tubing of the high-pressure homogenizer.

In conclusion, it can be seen that DPPC produces smaller nanoemulsion droplets in comparison to DMPC and DSPC. The

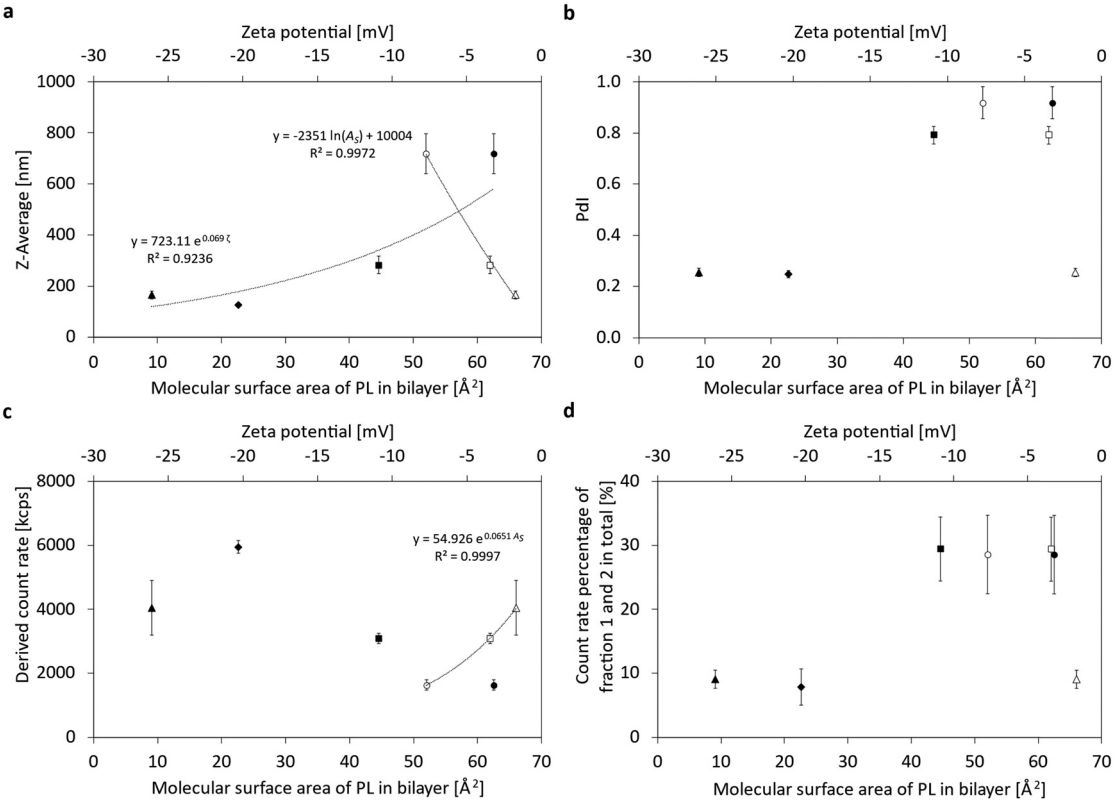

Fig. 5 Comparison of the phospholipid head groups DPPE (● ○), DPPC (■ □), DPPG (▲△) DPPA (◊) correlated to the molecular surface area of the phospholipid in a bilayer or correlated to the zeta potential. Open symbols indicate the ζ-potentials, while closed symbols indicate the respective molecular areas (A_S). Note that no literature reference exists for the molecular area of DPPA. (a) The *Z*-average (*Z*-Ave) after 6 cycles at 1000 bar without fractionation using a sucrose gradient, (b) the corresponding polydispersity index (PdI), (c) the corresponding derived count rate (DCR) of the PFC/W nanoemulsion and (d) the count rate percentages of fraction 1 and 2 after fractionation. The dots represent the mean values ± SD, n = 3.

PdI of DSPC is the lowest but this fact has to be seen in the context of a *Z*-Ave which is almost doubled compared to DPPC. The minimum droplet size of DPPC nanoemulsions is also reflected by a significantly increased derived count rate (DCR). The differences between DMPC, DPPC and DSPC can be interpreted with respect to their main transition temperature which allows DMPC liposomes to transform from the bilayer to the monolayer conformation with a liposomal residue of only about 13%, but due to the fluidity of its monolayer, droplet coalescence is much more likely, leading to larger droplets.

The results of the head group variation are summarized in Fig. 5 and Fig. S4 (ESI†). Varying the phospholipid head group reveals a logarithmic relationship between particle size (Fig. 5a) and the molecular area for bilayers of the phospholipid head groups of phosphatidylethanolamine (PE), phosphatidylcholine (PC), and phosphatidylglycerol (PG).[21] Bilayer molecular area data for free phosphate (PA) are not available. On a secondary *x*-axis, the correlation of the *Z*-Ave and the Zeta potential (ζ) is shown for all four head groups, DPPE, DPPC, DPPA and DPPG, together with an exponential regression. A linear regression is shown for the polydispersity index (PdI) and the ζ-potential of the four head groups (Fig. 5b), proving their correlation. Positive correlations are also found between the derived count rate (DCR) and the magnitude of the ζ-potential and the molecular area (Fig. 5c). Looking at the proportion of the remaining liposomes in Fig. 5d, the head groups can either be regarded in an exponential regression between F1 + F2 percentage *vs.* ζ-potential or by differentiating the relationship into two sub-groups: on the one hand, there are the zwitterionic phospholipids PE and PC, in which a high proportion of liposomes remain in the final nanoemulsion, and on the other hand, the anionic phospholipids PG and PA are presented against their ζ-potentials. In the case of DPPG and also DPPA, the proportion of the remaining liposomes is significantly lower, *i.e.* below 10%, which indicates that liposomal breakup is much more successful by high-pressure homogenization for phospholipids carrying repulsive charges.

In summary, it can be seen that droplet sizes decrease with increasing ζ-potential and increasing molecular area, the same trend is visible for the decreasing PdI with increasing potential. In contrast, DCR increases with increasing ζ-potential and increasing molecular area. Moreover, the percentage of liposomes persisting the transition into emulsifying monolayers can be assigned to two sub-groups: zwitterionic and anionic phospholipids, the former having high liposomal percentages of almost 30%, while the latter are clearly below 10%. Thus, higher ζ-potentials and molecular areas lead to lower particle sizes, lower PdI and smaller fractions of the remaining

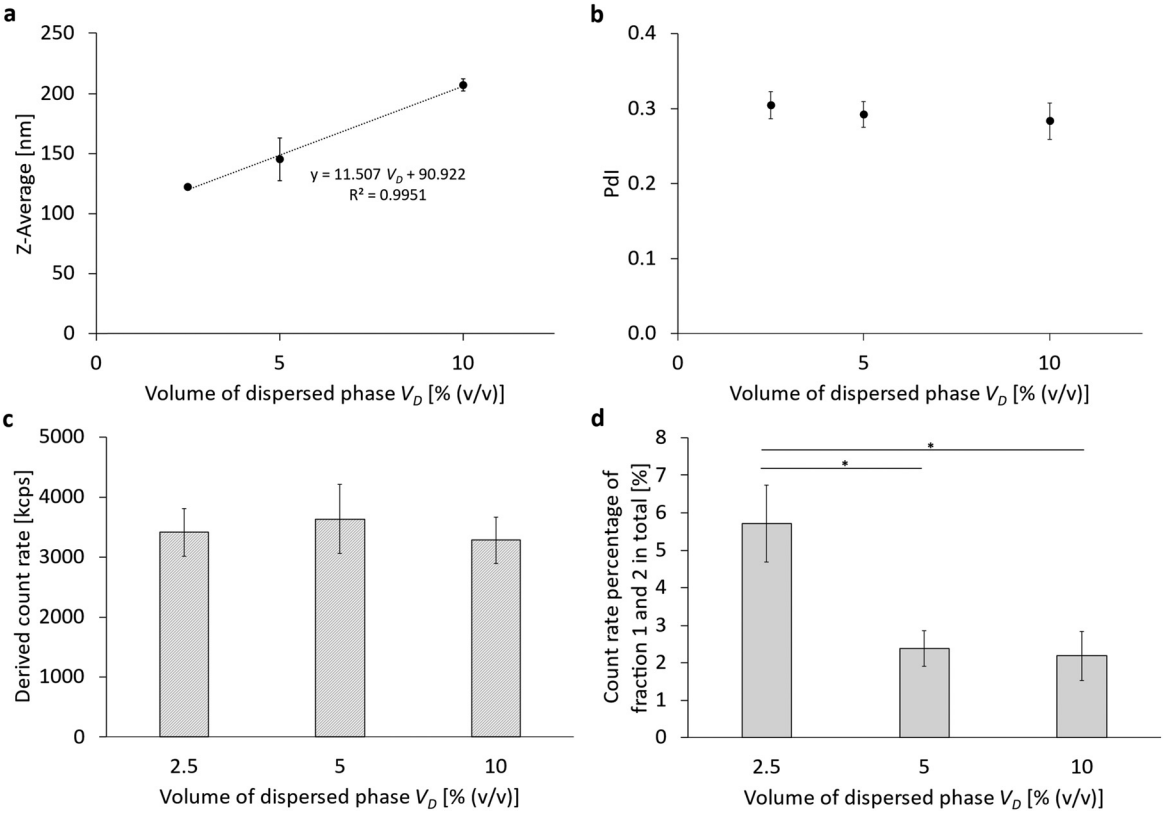

Fig. 6 Comparison of the different volume percentages of the perfluorocarbon as dispersed phase. (a) The *Z*-average (*Z*-Ave) after 6 cycles at 1000 bar without fractionation using a sucrose gradient, (b) the corresponding polydispersity index (PdI), (c) the corresponding derived count rate (DCR) of the PFC/W nanoemulsion and (d) the count rate percentages of fraction 1 and 2 after fractionation using a sucrose gradient. The bars or dots represent the mean values ± SD. A one-way ANOVA followed by a two-sample *t*-test assuming equal variances was performed at a significance level of $*p < 0.05$; $n = 3$.

liposomes. These facts indicate that stronger repulsive forces and steric hindrances lead to better emulsifying properties.

Experimental investigation of changes in the emulsion formulation with regard to the dispersed phase

Variation in the properties of the dispersed phase. In addition to the lipid composition and lipid concentration, it is of interest to vary the dispersed phase of the PFC/W nanoemulsion.

For this purpose, the volume fraction of the dispersed perfluorocarbon phase V_D was increased from V_D = 2.5% (v/v) to 5% (v/v) and up to V_D = 10% (v/v) (Table 1 and Fig. 2 part 5). Simultaneously, the lipid concentration c_L was kept constant at c_L = 7.5 mM, thus producing ratios of c_L/V_D = 3 mM; 1.5 mM; or 0.75 mM per 1% (v/v) of disperse phase. The results are summarized in Fig. 6 and Fig. S5 (ESI†). When looking at the particle size (Fig. 6a) after 6 cycles of homogenization at 1000 bar, a linear relationship between the *Z*-Ave and the proportion of the dispersed phase can be seen. Thus, the particle size increases with increasing PFC content. In contrast, the PdI (Fig. 6b) and the derived count rate (Fig. 5c) show no differences between the different proportions of the dispersed phase. Similarly, there is no difference in the proportion of the remaining liposomes between 5% (v/v) and 10% (v/v), but there is a maximum of the remaining liposomes at 2.5% (v/v) with 5.7% ± 1.0%.

Concerning the rheology of dilute emulsions or suspensions, the legendary publication by Einstein (1905) on Brownian motion shows that the volume fraction linearly influences the increase in viscosity. At higher volume fractions, non-linear terms influence the increase in the emulsion viscosities. Applying the three different theoretical approaches,[27–29] we could show that emulsion viscosity is increased by 6.3–6.6%, 12.5–13.9%, and 25–31.5% for a dispersed phase volume of 2.5, 5 and 10% (v/v), respectively. Details can be found in the ESI,† Table S8. This comparison allows two conclusions: (a) the maximum difference between linear and non-linear models for the dynamic viscosity of dilute suspensions with a dispersed phase fraction of 2.5% to 10% (v/v) is between 0.3 and 6.6% of the continuous phase's viscosity. (b) The increase of emulsion viscosity caused by 2.5% dispersed phase is roughly compensated by the decrease in viscosity caused by a single homogenization cycle causing a temperature increase by about 2.41 °C.

Thus, the results shown in Fig. 6 accurately complement the results from Fig. 3 which had proven an optimum of their particle size (*Z*-Ave) at a ratio of c_L/V_D = 2 mM per 1% (v/v) of disperse phase. Clearly, the particle size can be further decreased with an even higher ratio of c_L/V_D = 2 mM/1% (v/v), but this increases the excess amount of liposomes which are not transformed into emulsifying monolayers.

Table 3 Surface area depending on PFC volume percentage

Volume of dispersed phase V_D [% (v/v)]	Hypothetical surface area per molecule [Å^2 per molecule]
2.5	29.69
5	49.67
10	98.92

Table 3 shows the hypothetical surface area per lipid molecule for the varying amounts of the dispersed phase. Analogously to Table 2, it can be concluded that only for a PFC volume percentage of 10% (v/v), a pure monolayer is formed at the emulsions' phase boundaries. This corresponds to a ratio of c_L/V_D = 0.75 mM, while for c_L/V_D = 1.5 mM/1% (*i.e.* 5% PFC (v/v)), already an inhomogeneous monolayer–multilayer status must be reached, while for c_L/V_D = 3 mM/1% (*i.e.* 2.5% PFC (v/v)), a triple layer is formed.

Variation of the viscosity ratio of the continuous and dispersed phase using different perfluorocarbons. Perfluoroperhydrophenanthrene was used as the dispersed phase in all cases as shown in Fig. 1 and 3–6, which has a dynamic viscosity η of 28.4 mPa s (Table 4), resulting in a viscosity ratio of continuous to dispersed phase of almost 1 : 30. For this reason, the viscosity of the dispersed phase was tested in a further series of experiments by changing the perfluorocarbon (Table 1 and Fig. 2 part 6). Table 4 lists the dynamic viscosities as well as the boiling points and densities ρ of the perfluorocarbons used. The limited availability of perfluorocarbons limits the adjustment of viscosity ratios.

The results of varying the viscosity of the dispersed phase are summarized in Fig. 7 and Fig. S6 (ESI†). For the *Z*-averaged particle size (Fig. 7a), the polydispersity index PdI (Fig. 7b) and the count rate percentage of the remaining liposomes (Fig. 7d), a linear correlation of the respective parameter with the increasing viscosity of the cyclic perfluorocarbons is shown. Only the derived count rate of the PFC/W nanoemulsion before separation in the sucrose gradient shows a logarithmically decreasing correlation between the DCR and the increasing viscosity of the cyclic perfluorocarbons. As can be seen, the linear PFCs deviate from the correlations for cyclic perfluorocarbons. Minor deviations occur for the *Z*-Ave (Fig. 7a) and PdI (Fig. 7b), but larger deviations are visible for the derived count rate (Fig. 7c) and count rate percentage of non-transformed liposomes (Fig. 7d).

Table 4 Overview of various physicochemical properties of the perfluorocarbons used, such as boiling point, density and viscosity, as well as the corresponding structural formula

Name	Boiling point [°C]	Density ρ at 25 °C [g mL^{-1}]	Dynamic viscosity η at 25 °C [mPa s]	Structure
Perfluoroheptane	82	1.72	0.9	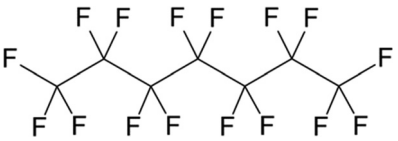
Perfluoro-1,3-dimethylcyclohexane	102	1.83	1.9	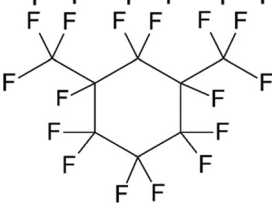
Perfluorooctyl bromide	141–143	1.93	2.3	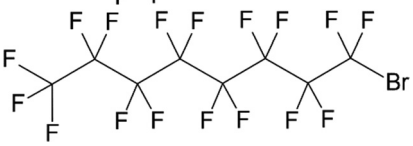
Perfluorodecalin	142	1.94	5.1	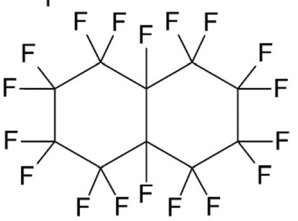
Perfluoroperhydro-phenanthrene	215	2.03	28.4	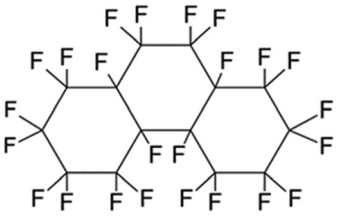

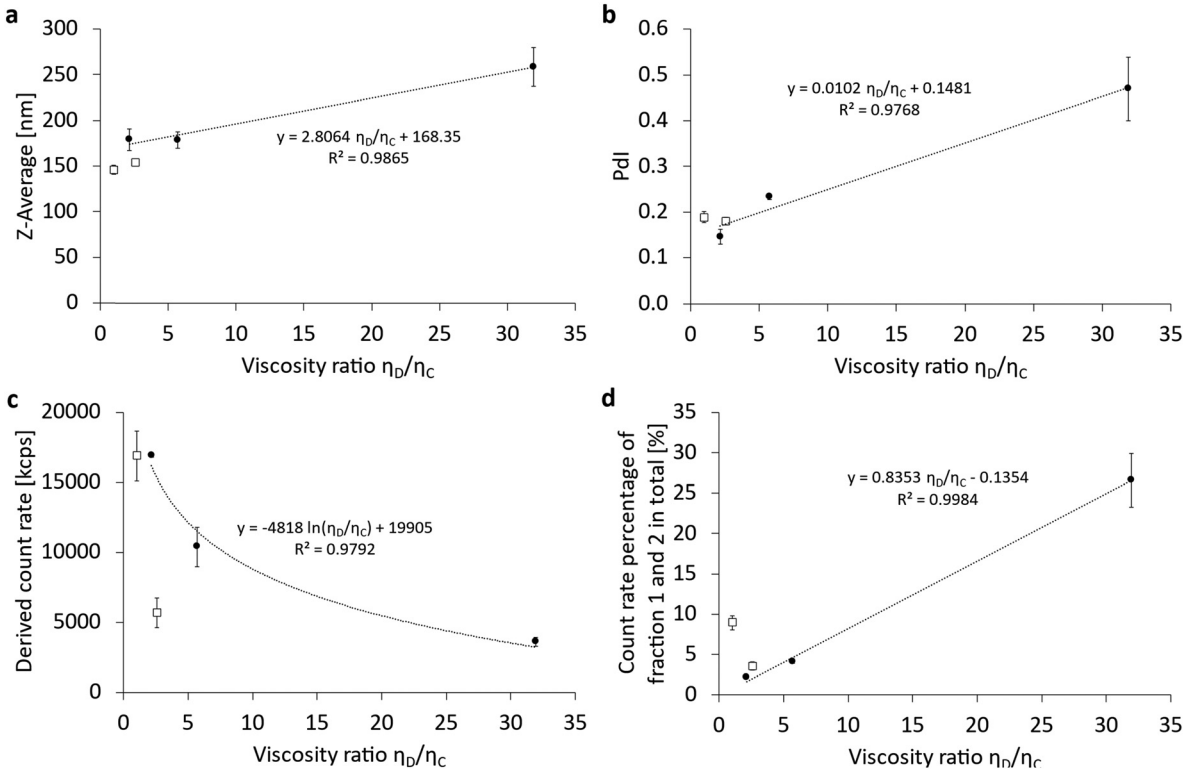

Fig. 7 Comparison of the different viscosity ratios of the dispersed phase to the continuous phase by varying the perfluorocarbon, sub-classified as linear (□) and cyclic (●) perfluorocarbons (PFC) with all regressions shown corresponding only to the cyclic PFC. The continuous phase consisted of water with a dynamic viscosity of 0.89 mPa s at 25 °C. (a) The *Z*-average (*Z*-Ave) after 6 cycles at 1000 bar without fractionation using a sucrose gradient, (b) the corresponding polydispersity index (PdI), (c) the corresponding derived count rate (DCR) of the PFC/W nanoemulsion and (d) the count rate percentages of fraction 1 and 2 after fractionation using a sucrose gradient. The dots represent the mean ± SD, n = 3.

The dependency of emulsification on the viscosity ratio of dispersed and continuous phases was studied for various practical applications in the last decades.[22,30–34] However, most studies focus on emulsion droplets in the micrometer range with the exception of the study by Qian and McClements (2011).[22] Moreover, none of the prior studies have used phospholipids as emulsifiers, even though their properties are decisive as demonstrated by Qian and McClements.[22] They made a comparison of β-lactoglobulin and sodium dodecyl sulfate (SDS) with the former having no size increase with increasing viscosity ratio, while the latter increases with a power law exponent of 0.2271.[22] Comparing our data with those by Qian and McClements[22] concerning the increase of the *Z*-averaged droplet size, we find a linear correlation. In absolute numbers, our minimum and maximum viscosity ratios η_D/η_C (1.0 *vs.* 31.9) shown in Fig. 6a differ in their respective *Z*-Ave between 179 nm ± 12 nm and 259 nm ± 21 nm, thus showing a relative size increase of 44%. For the same viscosity ratios η_D/η_C (1.0 *vs.* 31.9), the increase in *Z*-Ave would have been 219% for SDS as an emulsifier according to the assessment shown by Qian and McClements (2011).[22] This comparison shows that the emulsifying properties of dispersed phases follow 2 mechanisms:

1. The molecular weight of the emulsifier dictates if the mean droplet sizes show a dependency on the viscosity ratio of dispersed and continuous phases η_D/η_C. β-Lactoglobulin (M_w: 19.9 kDa) shows no significant size difference with varying η_D/η_C, while egg phospholipid E80 with 40 mol% cholesterol (averaged M_w: 617 Da) has a mild dependency. In contrast, SDS (M_w: 288 Da) exhibits a stronger dependency in the same viscosity ratio range.

2. In case the emulsifier allows droplet size differences depending on the viscosity ratio, higher η_D/η_C produces larger average droplet sizes.

This comparison shows that the mechanical properties of both the emulsifier and the bulk phases' viscosities influence high-pressure emulsification. The influence of the emulsifier has higher priority, as the example of β-lactoglobulin shows, indicating that overcoming the mechanical resistance of the emulsifying mono- or multi-layer is the main key for successful droplet size minimization. Ruptures of emulsifying layers obviously lead to direct droplet break-up, irrespective of the resistance of a high-viscosity dispersed phase. In contrast, emulsifiers of very low surface viscosities and elasticities are dominated by the bulk viscosity of the dispersed phase.

In summary, it can be noted that the averaged particle sizes of emulsification by phospholipids are affected by the viscosity ratio η_D/η_C leading to a mild increase in size with the growing viscosity of the dispersed phase. A similar effect also occurs for the PdI due to the increase in viscosity for cyclic PFCs of higher

molar weight. The DCR is strongly affected by the increase in the viscosity ratio η_D/η_C of the cyclic PFCs. Moreover, linear PFCs seem to have an even stronger dependency on the viscosity ratio, but this effect could also be specific to perfluorooctyl bromide and would need additional linear PFCs to be confirmed. The count rate percentage of persistent liposomal bilayers not transformed into emulsifiers is also strongly dependent on the viscosity ratio η_D/η_C. Here, linear PFCs also show different characteristics where the properties of perfluorooctyl bromide cannot be differentiated from those of the cyclic PFCs.

Conclusions

Our investigations allow several generalizations and conclusions to be made. In the case of the cholesterol content added to the natural blend of egg phosphatidylcholine (E80), an increase in droplet size (*Z*-Ave) can be observed with increasing cholesterol content $x_{chol} > 10$ mol%. A general statement can also be made concerning the lipid concentration c_L, as an optimum was found at 5 mM. In combination with the dispersed phase volume fraction V_D used, it results in an optimum ratio of c_L/V_D of 2 mM per 1% (v/v). Through the calculation of the mean area per molecule, we show that emulsification is only in a monolayer conformation for c_L/V_D = 1 mM/1% (v/v) but forms inhomogeneous or homogeneous multilayers for $c_L/V_D \geq 2$ mM/1% (v/v).

This ratio and the conclusions about monolayers *vs.* triple layers forming at the PFC/water interfaces were also confirmed in our studies on the dispersed phase volume fraction. For the dispersed volume V_D, it can generally be stated that an increasing V_D leads to an increase in particle size without influencing the PdI and the DCR. Through the calculation of the mean area per molecule and comparing it to the literature, we show that emulsification is only in a monolayer conformation for c_L/V_D = 1 mM/1% (v/v) but forms an inhomogeneous mixture of mono and triple layers or homogeneous triple layers for $c_L/V_D \geq 2$ mM/1% (v/v).

Concerning the selection of the specific phospholipid composition as an emulsifier, the following conclusions can be made for the fatty acid chain lengths: DPPC consisting of the two saturated fatty acids with 16 carbons without double bonds (16 : 0; 16 : 0) generates the smallest nanoemulsion droplets compared to DMPC (14 : 0; 14 : 0) and DSPC (18 : 0; 18 : 0) and moreover has a significantly increased DCR. These effects can be correlated to the transition temperature which for DMPC allows re-coalescence of newly formed nanodroplets under processing temperatures (>25 °C) but remaining below DPPC main transition (41 °C). Durable mechanical break-up and droplet atomization are therefore optimized for fatty acids closely below their main transition temperature. Concerning phospholipid head groups, the following mechanisms can be observed: increasing ζ-potential and increasing molecular surface area of the phospholipid in a bilayer result in droplet size decreases and elevated derived count rates (DCR). Concerning the emulsification efficiency, phospholipid head groups can be divided into two subgroups: zwitterionic phospholipids are significantly less effective in emulsification compared to anionic phospholipids.

When considering the viscosity of the dispersed phase η_D, normalized by the viscosity of the continuous phase η_C, a generalized statement can be made. For the particle size, the PdI and also the proportion of the remaining liposomes as a measure of emulsification efficiency, there is a linear correlation with increasing viscosity ratio η_D/η_C. Comparing the emulsification properties of phospholipids with other amphiphiles in the literature,[22] it can be shown that the emulsifier's molecular weight is decisive for a hierarchical combination of emulsification mechanisms. High molecular weight (M_w) emulsifiers are not dependent on η_D/η_C, while smaller molecular weight compounds like phospholipids show a mild increase with growing η_D/η_C. In contrast, low molecular detergents like sodium dodecyl sulfate exhibit a stronger dependency on η_D/η_C. These examples show that overcoming the mechanical resistance of the emulsifier is the main key to successful droplet size minimization. Ruptures of emulsifying interfacial layers obviously lead to direct droplet break-up, irrespective of the resistance of a high-viscosity droplet. Thus, the lower the surface viscosities and elasticities of an emulsifier, the more is break-up of droplets governed by the bulk viscosity of the dispersed phase. Finally, it should be noted that the correlations found for different chemical species of perfluorocarbons only apply to cyclic perfluorocarbons, while linear PFCs do not always follow these correlations.

Author contributions

Larissa L. Lubitz: conceptualization, methodology, validation, formal analysis, investigation, writing – original draft, visualization. Harden Rieger: resources, writing – review & editing. Gero Leneweit: conceptualization, project coordination, funding acquisition, supervision, writing – review & editing. All authors reviewed the manuscript.

Data availability

The data supporting this article have been included as part of the ESI.†

Conflicts of interest

The authors declare that they have no known competing financial interests or personal relationships that could have appeared to influence the work reported in this article.

Acknowledgements

The RELIEF project (E! 113670) has received funding from the Eurostars-2 joint program with co-funding from the European Union Horizon 2020 research and innovation program. It is sponsored by the Bundesministerium für Bildung und Forschung (01QE2008A). The authors acknowledge support from

Moritz P. Haffner, Lisa Klingel and Ulf Garbe in conducting the experiments and collecting the data.

References

1 P. Marie, J. M. Perrier-Cornet and P. Gervais, *J. Food Eng.*, 2002, **53**, 43–51.
2 G. Kolb, K. Viardot, G. Wagner and J. Ulrich, *Chem. Eng. Technol.*, 2001, **24**, 293–296.
3 S. Schultz, G. Wagner, K. Urban and J. Ulrich, *Chem. Eng. Technol.*, 2004, **27**, 361–368.
4 P. L. Luisi, R. Scartazzini, G. Haering and P. Schurtenberger, *Colloid Polym. Sci.*, 1990, **268**, 356–374.
5 J. H. Sommerling, M. B. C. De Matos, E. Hildebrandt, A. Dessy, R. J. Kok, H. Nirschl and G. Leneweit, *Langmuir*, 2018, **34**, 572–584.
6 J. G. Riess and M. P. Krafft, *Biomaterials*, 1998, **19**, 1529–1539.
7 H. Träuble and E. Grell, *Neurosci. Res. Program Bull.*, 1971, **9**, 373–380.
8 S. Pautot, B. J. Frisken and D. A. Weitz, *Proc. Natl. Acad. Sci. U. S. A.*, 2003, **100**, 10718–10721.
9 A. D. Bangham, M. M. Standish and J. C. Watkins, *J. Mol. Biol.*, 1965, **13**, 238–252.
10 J.-P. Colletier, B. Chaize, M. Winterhalter and D. Fournier, *BMC Biotechnol.*, 2002, **2**, 9.
11 T. Zhang, Q. Zhang, J. H. Tian, J. F. Xing, W. Guo and X. J. Liang, *MRS Commun.*, 2018, **8**, 303–313.
12 F. Szoka and D. Papahadjopoulos, *Proc. Natl. Acad. Sci. U. S. A.*, 1978, **75**, 4194–4198.
13 K. Ullmann, G. Leneweit and H. Nirschl, *Pharmaceutics*, 2021, **13**(5), 691.
14 E. Hildebrandt, J. H. Sommerling, G. Guthausen, K. Zick, J. Stürmer, H. Nirschl and G. Leneweit, *Colloids Surf., A*, 2016, **505**, 56–63.
15 A. M. Tikhonov, *JETP Lett.*, 2020, **131**, 714–722.
16 M. Adamczak, G. Para, C. Simon and P. Warszyński, *J. Microencapsulation*, 2013, **30**, 479–489.
17 Y. Shao, C. Zhang, Q. Yao, Y. Wang, B. Tian, X. Tang and Y. Wang, *Eur. J. Pharm. Sci.*, 2014, **52**, 1–11.
18 D. Needham and R. S. Nunn, *Biophys. J.*, 1990, **58**, 997–1009.
19 C. Kirby, J. Clarke and G. Gregoriadis, *Biochem. J.*, 1980, **186**, 591–598.
20 T. Nii and F. Ishii, *Colloids Surf., B*, 2005, **41**, 305–311.
21 J. H. Kleinschmidt and L. K. Tamm, *Biophys. J.*, 2002, **83**, 994–1003.
22 C. Qian and D. J. McClements, *Food Hydrocolloids*, 2011, **25**, 1000–1008.
23 S. Tesch and H. Schubert, *J. Food Eng.*, 2002, **52**, 305–312.
24 O. Behrend, K. Ax and H. Schubert, *Ultrason. Sonochem.*, 2000, **7**, 77–85.
25 L. Lubitz, H. Rieger and G. Leneweit, *Sci. Rep.*, under revision.
26 Y. Klapper, M. Vrânceanu, Y. Ishitsuka, D. Evans, D. Scheider, G. U. Nienhaus and G. Leneweit, *J. Colloid Interface Sci.*, 2013, **390**, 267–274.
27 A. Einstein, *Ann. Phys.*, 1905, **322**, 549–560.
28 E. Guyon, J. P. Hulin, L. Petit and C. D. Mitescu, *Physical Hydrodynamics*, Oxford University Press, 2015.
29 I. M. Krieger and T. J. Dougherty, *Trans. Soc. Rheol.*, 1959, **3**, 137–152.
30 W. D. Pandolfe, *J. Dispersion Sci. Technol.*, 1981, **2**, 459–474.
31 M. Briceño, J. L. Salager and J. Bertrand, *Chem. Eng. Res. Des.*, 2001, **79**, 943–948.
32 C.-O. Fournier, L. Fradette and P. A. Tanguy, *Eng. Res. Des.*, 2009, **87**, 499–506.
33 L. Hohl, S. Röhl and M. Kraume, *Chem. Eng. Technol.*, 2023, **46**, 1260–1270.
34 F. Lewerentz, K. Pappas, B. Bergenståhl and A. Håkansson, *Food Bioprod. Process.*, 2023, **138**, 103–115.

